THE GEOLOGICAL SOCIETY OF AMERICA

Geological Society of America
3300 Penrose Place
P.O. Box 9140
Boulder, CO 80301
(303) 447-2020 • fax 303-357-1073
www.geosociety.org

This PDF file is subject to the following conditions and restrictions:

Copyright © 2006, The Geological Society of America, Inc. (GSA). All rights reserved. Copyright not claimed on content prepared wholly by U.S. government employees within scope of their employment. Individual scientists are hereby granted permission, without fees or further requests to GSA, to use a single figure, a single table, and/or a brief paragraph of text in other subsequent works and to make unlimited copies for noncommercial use in classrooms to further education and science. For any other use, contact Copyright Permissions, GSA, P.O. Box 9140, Boulder, CO 80301-9140, USA, fax 303-357-1073, editing@geosociety.org. GSA provides this and other forums for the presentation of diverse opinions and positions by scientists worldwide, regardless of their race, citizenship, gender, religion, or political viewpoint. Opinions presented in this publication do not reflect official positions of the Society.

Geological Society of America
Special Paper 410
2006

New U-Pb radiometric dates of the Bear Mountain intrusive complex, Klamath Mountains, California

Kevin R. Chamberlain*
Arthur W. Snoke
Department of Geology and Geophysics, Department 3006,
1000 East University Avenue, University of Wyoming, Laramie, Wyoming 82071, USA
Calvin G. Barnes
Department of Geosciences, Texas Tech University, Lubbock, Texas 79409-1053, USA
Jonathan C. Bushey
Department of Geology and Geophysics, Department 3006,
1000 East University Avenue, University of Wyoming, Laramie, Wyoming 82071, USA

ABSTRACT

New, high-precision U-Pb titanite (sphene) and zircon dates from five samples of the Bear Mountain intrusive complex establish the timing and duration of magmatism. The oldest, magmatic date (150.5 ± 0.6 Ma) comes from dark-colored titanite from a biotite-hornblende tonalite that is part of a composite pluton that intrudes the Blue Ridge ultramafic-gabbroic intrusion. Pale titanite and zircon from this sample yielded a distinctly younger date of 149.3 ± 0.3 Ma. A similar pattern of mineral dates is also apparent in two samples of the areally extensive Punchbowl unit of the Bear Mountain pluton. Dark-colored titanite in one of these samples yielded a date of 149.5 ± 0.6 Ma, whereas the dates of pale titanite and zircon are 147.4 ± 0.3 Ma. The second sample of the Punchbowl unit only contained a single morphology of pale titanite, which yielded the same date as zircon (148.2 ± 0.3 Ma). The U-Pb zircon date of the Buck Lake unit of the Bear Mountain pluton, 148.2 ± 0.2 Ma, supports field evidence that the Buck Lake unit was emplaced synchronously with the Punchbowl unit. A lower age limit on magmatism in the Bear Mountain intrusive complex comes from a 145.4 ± 0.4-Ma zircon date from a late crosscutting mafic dike. All samples exhibit slight inheritance in the zircon data, with 152- to 150-Ma minimum ages. The mafic dike contains inherited components that are at least 264 Ma and possibly Paleoproterozoic in age.

The new dates constrain magmatism in the Bear Mountain intrusive complex to the period from 151 to 147 Ma, with a minimum duration of 1.5 m.y. and a maximum of 6 m.y. The dates establish that the emplacement and crystallization of the Bear Mountain intrusive complex post-dated regional thrust faulting (Orleans fault) associated with the Nevadan orogeny, including the South Siskiyou Fork fault, which is interpreted as an oblique-slip tear fault associated with the Orleans (thrust) fault system.

*E-mail: kchamber@uwyo.edu.

Chamberlain, K.R., Snoke, A.W., Barnes, C.G., and Bushey, J.C., 2006, New U-Pb radiometric dates of the Bear Mountain intrusive complex, Klamath Mountains, California, *in* Snoke, A.W., and Barnes, C.G., eds., Geological studies in the Klamath Mountains province, California and Oregon: A volume in honor of William P. Irwin: Geological Society of America Special Paper 410, p. 317–332, doi: 10.1130/2006.2410(15). For permission to copy, contact editing@geosociety.org.
©2006 Geological Society of America. All rights reserved.

The pattern of mineral dates from the composite pluton intruded into the Blue Ridge intrusion as well as the areally more extensive Punchbowl unit indicate that crystallization of these bodies occurred over 1.5–2 m.y., due to either insulating effects of the intrusive complex and/or magma recharge.

Keywords: Klamath Mountains, northwestern California, Jurassic, U-Pb geochronology, titanite, zircon, igneous rocks, oceanic-arc pluton, thrust faulting, Nevadan orogeny

INTRODUCTION

The tectonic development of the Klamath Mountains province involved multiple contractional events, which led to the progressive accretion of predominantly oceanic terranes onto the western North American continental margin (Irwin, 1972, 1981; Harper and Wright, 1984; Harper et al., 1994; Irwin and Wooden, 1999; Fig. 1). Many of these tectonostratigraphic terranes represent parts of oceanic to near-continental arc sequences subsequently intruded by plutonic magmas that ranged from ultramafic to silicic. Some of these plutons are "pinning plutons" (after the terminology of Howell et al., 1985) that intrude across regional, terrane-bounding faults, whereas other plutons are truncated by regional faults. Thus, precise dating of these plutons provides important constraints on the timing and duration of tectonic activity within the Klamath Mountains province (e.g., Lanphere et al., 1968; Davis et al., 1978; Irwin, 1985; Wright and Fahan, 1988; Irwin and Wooden, 1999).

One of the most important and widespread contractional events in the Klamath Mountains province was thrusting of terranes of the western Paleozoic and Triassic belt (Irwin, 1972) over terranes of the western Jurassic belt (Blake, 1984; Blake et al., 1985). This event typically emplaced higher-grade rocks of the hanging-wall allochthon onto lower-grade rocks of the footwall along the east-rooted, west-directed Orleans fault (Hershey, 1906, 1911), a regional thrust fault with a minimum horizontal displacement of ~70 km (Jachens et al., 1986). In the central Klamath Mountains, the age of thrusting is constrained by ca. 153-Ma detrital zircon ages in footwall rocks of the Galice Formation (Miller et al., 2003) and the ca. 150-Ma Summit Valley "pinning pluton" (Harper et al., 1994). This orogenic event (commonly referred to as the "Nevadan orogeny"; Blackwelder, 1914; Taliaferro, 1942; Snoke and Barnes, this volume) also involved polyphase folding of the metasedimentary rocks of the footwall (Upper Jurassic Galice Formation; e.g., Snoke, 1977; Harper and Wright, 1984; Harper et al., 1994; Gray, this volume).

The Bear Mountain intrusive complex consists of two large plutons, a number of smaller intrusive bodies, and associated dikes (Snoke et al., 1981; Bushey et al., this volume). The large proportion of ultramafic and gabbroic to dioritic rocks that comprise the Bear Mountain intrusive complex suggests that this intrusive complex is the underpinnings of a primitive oceanic arc (Snoke et al., 1981, 1982). Initial U-Pb zircon radiometric dating of the Bear Mountain intrusive complex (Saleeby et al., 1982) yielded Late Jurassic (i.e., Nevadan) ages. Specifically, Saleeby et al. (1982) reported ages as old as ca. 153 Ma and as young as ca. 149 Ma. As the timing of thrusting on the Orleans fault was refined, it became apparent that these U-Pb zircon dates suggested a syn-thrusting emplacement history for the Bear Mountain intrusive complex. This chapter reports the results of high-precision dating of zircon and titanite (sphene) from several intrusive units in the Bear Mountain intrusive complex. The data are interpreted to suggest that the intrusive complex was emplaced immediately after thrusting ended, although field and petrographic evidence indicates that deformation continued during the emplacement of the intrusive complex. These new data also indicate a protracted (several m.y.) magmatic history of the Bear Mountain intrusive complex, which has important implications for the longevity of magmatism in arc-related settings.

GEOLOGIC SETTING

At the present level of exposure, the Bear Mountain intrusive complex intrudes the Rattlesnake Creek terrane, including the late Middle Jurassic (ca. 164 Ma) mafic complex of the Preston Peak ophiolite (Snoke, 1977; Saleeby et al., 1982; Harper et al., 1994). Furthermore, the Bear Mountain pluton truncates the Twin Peaks fault, a north–south-striking fault that separates the rocks of the mafic complex on the west side of the fault (footwall) from serpentinized peridotite of the basement complex of the Rattlesnake Creek terrane on the east side (hanging wall) of the fault (Fig. 2). This fault is interpreted as a high-angle, reverse fault related to the Orleans fault system (Preston Peak fault [thrust] of Snoke, 1977), the terrane-bounding fault that separates the Rattlesnake Creek terrane from the western Klamath terrane, including the Upper Jurassic Galice Formation (Fig. 1). In the same light, the Bear Mountain intrusive complex truncates the northwest–southeast-striking, South Siskiyou Fork fault (Snoke, 1977; Fig. 2) that is interpreted as a tear fault

Figure 1. Generalized geologic map of the Klamath Mountains province. BMic—Bear Mountain intrusive complex; BPic—Bear Peak intrusive complex (see McFadden et al., this volume); O. ft.—Orleans fault. The Preston Peak fault of Snoke (1977) is the local name for the regional Orleans (thrust) fault. Modified from Irwin (1994).

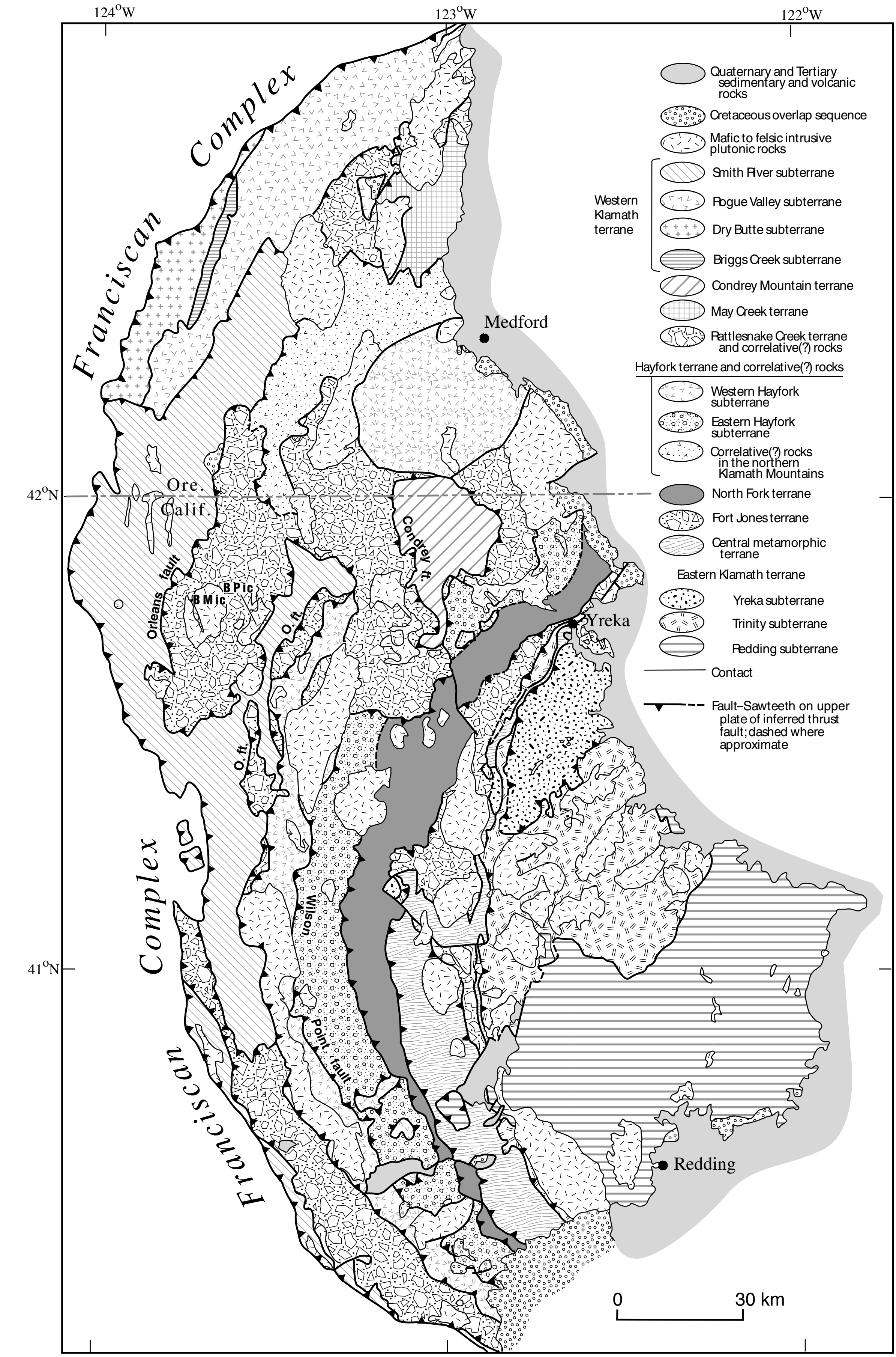
124°W
123°W
122°W
42°N
41°N
Franciscan Complex
Franciscan Complex
Medford
Ore.
Calif.
Orleans fault
BPic
BMic
O. ft.
O. ft.
Condrey ft.
Yreka
Wilson Point fault
Redding
0
30 km
Quaternary and Tertiary sedimentary and volcanic rocks
Cretaceous overlap sequence
Mafic to felsic intrusive plutonic rocks
Western Klamath terrane
Smith River subterrane
Rogue Valley subterrane
Dry Butte subterrane
Briggs Creek subterrane
Condrey Mountain terrane
May Creek terrane
Rattlesnake Creek terrane and correlative(?) rocks
Hayfork terrane and correlative(?) rocks
Western Hayfork subterrane
Eastern Hayfork subterrane
Correlative(?) rocks in the northern Klamath Mountains
North Fork terrane
Fort Jones terrane
Central metamorphic terrane
Eastern Klamath terrane
Yreka subterrane
Trinity subterrane
Redding subterrane
Contact
Fault–Sawteeth on upper plate of inferred thrust fault; dashed where approximate

associated with the Orleans fault (see Bushey et al., this volume, for a more detailed discussion of the field relationships). These field relationships thus suggest that the Bear Mountain intrusive complex was emplaced after tectonic juxtaposition of the Rattlesnake Creek terrane above the western Klamath terrane. The age of the Upper Jurassic Galice Formation, which is widespread and the stratigraphically highest unit in the western Klamath terrane, is based on the presence of the pelecypod *Buchia concentrica* (Sowerby), which ranges from the late Oxfordian to middle Kimmeridgian (Imlay, 1959) and the presence of ca. 153-Ma detrital zircon grains (Miller et al., 2003).

The contact-metamorphic effects in the country rocks surrounding the Bear Mountain intrusive complex are widespread and locally intense (Snoke et al., 1981; Bushey et al., this volume). Rocks of the Rattlesnake Creek terrane commonly reached hornblende-hornfels–facies conditions in the inner aureole of the Bear Mountain intrusive complex and locally reached pyroxene-hornfels–facies conditions (two-pyroxene–bearing mafic rocks; Fig. 2). The rocks of the inner aureole are chiefly hornblende schists or fine-grained amphibolite with a pervasive foliation and commonly a steeply plunging mineral lineation, defined by hornblende grains. Subordinate metasedimentary rocks (chiefly siliceous meta-argillite) are intercalated with the metabasic rocks of the inner aureole. Some of the metabasic rocks of the Rattlesnake Creek terrane were partially melted in the inner aureole, yielding migmatitic amphibolites with tonalitic leucosomes (Snoke and Barnes, 2002).

The Bear Mountain intrusive complex was initially subdivided into five broad lithologic units based chiefly on petrography (Snoke et al., 1981): (1) ultramafic and gabbroic rocks of the Blue Ridge intrusion, other small ultramafic intrusive bodies, and related dikes; (2) biotite–two-pyroxene monzodiorite/diorite; (3) heterogeneous hornblende-rich gabbro and diorite and related dikes; (4) leucocratic rocks, chiefly biotite ± hornblende tonalite and granodiorite; and (5) late dikes (mafic to felsic). Field relationships, including the contact metamorphism of clinopyroxenitic dikes of unit 1 by unit 2, indicate that the Blue Ridge intrusion and other satellitic ultramafic-gabbroic bodies are the oldest units of the intrusive complex. Leucocratic rocks intrude all other units except the late dikes; however, it was not clear whether these leucocratic rocks represented a single stage of magmatism or encompassed the entire Bear Mountain intrusive complex time interval. Relative relationships between units 2 and 3 were much more equivocal, but Snoke et al. (1981) concluded that unit 2 was older than unit 3. Recent geologic mapping by Bushey et al. (this volume) has revised these subdivisions, particularly in regard to units 2 and 3. These authors designate three plutonic units in the northern part of the Bear Mountain pluton: Buck Lake, Punchbowl, and Doe Flat. The Buck Lake unit is basically equivalent to unit 2 of Snoke et al. (1981), whereas the Punchbowl and Doe Flat units are unit 3 of Snoke et al. (1981). Bushey et al. (this volume) cite specific field relationships, including crosscutting dikes and inclusions of one unit within another, that indicate that the Doe Flat unit is younger than either the Buck Lake or Punchbowl units, whereas field relationships between the latter two units suggest a rough synchronicity. The new geochronological data presented in this chapter support this basic chronology.

URANIUM-LEAD GEOCHRONOLOGY

Five samples were collected from the Bear Mountain intrusive complex to determine the crystallization ages of different intrusive phases and overall duration of magmatism in the intrusive complex. The samples include a biotite-hornblende tonalite (DP2-20z) that is part of a small, composite pluton emplaced into the Blue Ridge intrusion (Fig. 2); two samples from the Punchbowl unit (Bushey et al., this volume), a predominantly hornblende-pyroxene gabbro-diorite (DP4-8z and 10z); a biotite–two-pyroxene diorite from the Buck Lake unit (DP1-13z) previously dated by Saleeby et al. (1982); and a late, undeformed crosscutting mafic dike (DP1-35z) that provides a lower age limit on magmatic activity during the development of the Bear Mountain intrusive complex.

Zircons were recovered and analyzed from each of these samples, and three of them also contained magmatic titanite (sphene). The titanite data are particularly useful, for titanite typically exhibits neither significant Pb loss nor inherited xenocrystic cores (e.g., Frost et al., 2001), both of which can add significant complexity in the interpretation of zircon data. The majority of the zircon analyses come from air-abraded grains, but some unabraded grains were also analyzed to test for metamorphic overgrowths and to monitor the overall effect of air abrasion on discordance. Two zircon fractions were analyzed by the annealing and partial dissolution method of Mattinson (2005), termed "chemical abrasion thermal ionization mass spectrometry," or CA-TIMS. This method is touted to reduce Pb loss effects in young zircons more effectively than simple mechanical abrasion. Sample locations are shown in Figure 2; data are presented in Tables 1 and 2. Laboratory procedures are described in Table 1. Concordia coordinates and radiogenic ages of individual analyses were calculated by using model mantle Pb isotopic values for 150 Ma (Zartman and Doe, 1981) for initial Pb and assigning variation in these values that approximates the range of modern-day measured mid-ocean ridge basalt (MORB). Model values were used rather than measured isotopic compositions of coexisting feldspars, because the samples had little to no alkali feldspar and measurements of plagioclase are typically slightly radiogenic, due to in situ decay of uranium. For Jurassic rocks, $^{206}Pb/^{238}U$ dates are generally the most reliable, and using a slightly radiogenic plagioclase $^{206}Pb/^{204}Pb$ value would lead to an age bias. These considerations only

Figure 2. Geologic map of the Bear Mountain intrusive complex. Sample locations for geochronology are indicated. Modified from Snoke et al. (1981); Bushey et al. (this volume); A.W. Snoke (unpublished data).

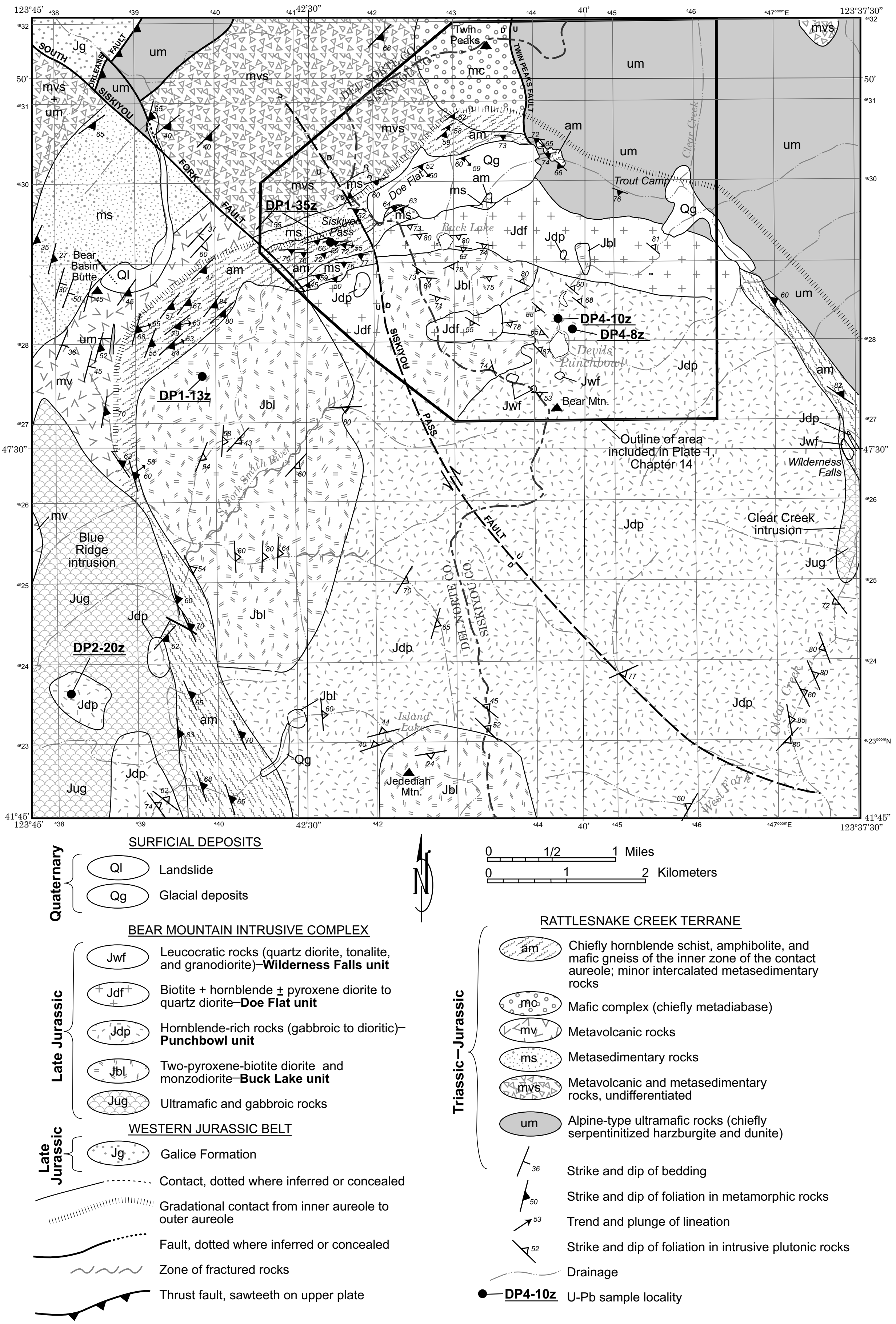

123°45'
42'30"
40'
123°37'30"
50'
47'30"
41°45'
SOUTH FORK FAULT
ORLEANS FAULT
SISKIYOU PASS FAULT
TWIN PEAKS FAULT
DEL NORTE CO.
SISKIYOU CO.
Twin Peaks
Doe Flat
Siskiyou Pass
Buck Lake
Trout Camp
Clear Creek
Devils Punchbowl
Bear Mtn.
Bear Basin Butte
S. Fork Smith River
Wilderness Falls
Clear Creek intrusion
Blue Ridge intrusion
Island Lake
Jedediah Mtn.
West Fork
DP1-35z
DP1-13z
DP4-10z
DP4-8z
DP2-20z
Outline of area included in Plate 1, Chapter 14
0 1/2 1 Miles
0 1 2 Kilometers
N
SURFICIAL DEPOSITS
Quaternary
Ql Landslide
Qg Glacial deposits
BEAR MOUNTAIN INTRUSIVE COMPLEX
Late Jurassic
Jwf Leucocratic rocks (quartz diorite, tonalite, and granodiorite)–Wilderness Falls unit
Jdf Biotite + hornblende ± pyroxene diorite to quartz diorite–Doe Flat unit
Jdp Hornblende-rich rocks (gabbroic to dioritic)–Punchbowl unit
Jbl Two-pyroxene-biotite diorite and monzodiorite–Buck Lake unit
Jug Ultramafic and gabbroic rocks
WESTERN JURASSIC BELT
Late Jurassic
Jg Galice Formation
Contact, dotted where inferred or concealed
Gradational contact from inner aureole to outer aureole
Fault, dotted where inferred or concealed
Zone of fractured rocks
Thrust fault, sawteeth on upper plate
RATTLESNAKE CREEK TERRANE
Triassic–Jurassic
am Chiefly hornblende schist, amphibolite, and mafic gneiss of the inner zone of the contact aureole; minor intercalated metasedimentary rocks
mc Mafic complex (chiefly metadiabase)
mv Metavolcanic rocks
ms Metasedimentary rocks
mvs Metavolcanic and metasedimentary rocks, undifferentiated
um Alpine-type ultramafic rocks (chiefly serpentinitized harzburgite and dunite)
36 Strike and dip of bedding
50 Strike and dip of foliation in metamorphic rocks
53 Trend and plunge of lineation
52 Strike and dip of foliation in intrusive plutonic rocks
Drainage
DP4-10z U-Pb sample locality

TABLE 1. DATA FOR U-Pb

Sample	Weight (mg)	U (ppm)	RadPb (ppm)	ComPb† (ppm)	Corrected atomic ratios§ $^{206}Pb/^{204}Pb$	%err	$^{238}U/^{204}Pb$	%err	$^{206}Pb/^{208}Pb$
DP2-20z bio-hbl tonalite (UTM S10 0438055E 4623651N)									
sphene							150.5 ± 0.61 Ma (MSWD = 0.0514) (3 pt.*		
sph nm1.0a lt 0.25mm	2.200	29	1.12	0.31	153.19	(1.1)	5774	(1.2)	3.03
sph nm1.0a dk 0.40mm*	2.250	77	5.37	2.01	74.74	(0.5)	2391	(0.7)	0.94
sph nm1.0a yel 0.25mm p1*	2.020	49	1.86	0.41	193.94	(1.0)	7438	(1.1)	2.55
sph nm1.0a yel 0.25mm p2*	1.950	49	1.82	0.36	217.32	(1.5)	8423	(1.7)	2.55
zircon							149.33 ± 0.29 Ma (MSWD = 1.3) (4 pt.* zr		
zr d-2 c'less euh*	0.046	56	2.51	1.10	92.20	(14)	3176	(18)	5.08
zr d-1 yel euh sm	0.028	118	3.03	0.22	776.59	(144)	33281	(147)	6.27
zr d-1 yel euh lg 7g	0.056	69	2.51	0.87	131.37	(16)	4942	(18)	6.32
zr d-2 yel euh sm aa*	0.129	32	1.02	0.21	245.20	(27)	9682	(30)	5.11
zr d-2 yel euh lg 24g aa*	0.167	83	2.01	0.02	5281	(207)	225237	(208)	6.72
zr d-2 yel euh lg 29g CA*	0.251	49	1.17	0.01	10336	(111)	440203	(112)	6.97
DP4-8z hbl-px gabbro (UTM S10 0444377E 4628108N)							149.5 ± 0.64 Ma 6/8 age one sphene pt.;		
zr d-1 pk anh sA	0.309	140	3.3	0.07	2968	(38)	128170	(38)	8.56
zr nm1 pk anh sB	0.144	144	3.5	0.10	2188	(56)	91454	(57)	10.38
zr d-1 yel anh sC aa*	0.334	221	5.2	0.00	508189	(3820)	21899000	(3820)	7.41
zr d-1 lt br anh sD aa*	0.446	83	1.9	0.01	15318	(228)	659810	(228)	11.13
zr d-1 yel anh sE aa*	0.520	294	6.9	0.06	7458	(27)	321820	(27)	7.84
zr d-1 yel anh sF aa	0.232	151	3.5	0.03	6252	(100)	273960	(100)	8.12
zr d-1 br anh sG aa*	0.844	387	9.4	0.12	4673	(7.9)	200780	(7.9)	6.70
sph nm1.0a dk 0.35mm 11g	1.410	88	4.5	0.64	218.72	(0.9)	8563	(0.9)	0.91
sph nm1.0a lt 0.20mm*	1.900	45	2.2	0.95	86.39	(0.4)	2940	(0.4)	2.62
DP4-10z hbl-px gabbro late pod (UTM S10 0444315E 4628198N)							148.24 ± 0.30 Ma (MSWD=0.94) (4 pt.*		
zr nm2 lt br anh sA	0.181	206	4.86	0.01	35299	(529)	1529150	(530)	7.33
zr nm2 lt br anh sB	0.013	1001	24.6	0.30	4864	(102)	205887	(102)	6.73
zr nm2 lt br anh 8g aa2*	0.743	24	0.62	0.03	1091	(32)	46122	(33)	6.34
zr nm2 lt br anh 24g aa*	0.102	143	4.26	0.57	380.20	(13)	15569	(14)	4.26
sph nm1.0a yel 0.35mm*	1.110	11	0.52	0.22	88.96	(2.6)	3057	(3.3)	3.02
sph nm1.0a yel 0.35mm p2*	4.440	64	2.28	0.49	202.96	(0.3)	7994	(0.6)	2.78
DP1-13z bio-2 px monzodiorite (UTM S10 0439716E 4627659N)							148.17 ± 0.21 Ma (MSWD = 0.92) (5 pt.*		
zr nm1 yel euh 5g	0.055	190	4.60	0.10	2688	(81)	115490	(81)	8.21
zr nm1 yel euh 6g aa*	0.055	183	4.51	0.18	1500	(92)	63892	(92)	7.27
zr nm2 yel euh 7g	0.055	220	5.37	0.11	2822	(143)	119910	(143)	7.31
zr d-1 yel anh incl. 36g aa*	0.186	112	2.73	0.07	2456	(64)	105040	(64)	6.97
zr d-1 yel euh 17g aa*	0.074	64	1.60	0.07	1414	(79)	60085	(79)	6.81
zr nm1 yel euh 25g aa2*	0.186	100	2.40	0.01	20555	(603)	881850	(603)	7.00
zr nm1 yel euh 7g CA*	0.278	94	2.25	0.01	17713	(91)	760950	(91)	7.06
DP1-35z late mafic dike (UTM S10 0441513E 4629247N)							≥145.43 ± 0.42 Ma (MSWD = 0.43) (2 pt.*		
zr nm2 yel euh 36g	0.052	537	12.61	0.56	1351	(31)	59839	(31)	8.21
zr nm2 yel euh 13g aa*	0.015	261	6.46	0.44	865	(121)	37196	(121)	7.76
zr nm3 yel euh 18g	0.051	266	6.52	0.12	3234	(144)	135130	(144)	7.85
zr d-1 yel euh 70g aa	0.074	194	4.64	0.16	1748	(66)	74909	(66)	9.04
zr nm2 yel euh incl. 65g aa	0.089	242	5.88	0.07	5403	(133)	224960	(133)	8.82
zr nm3 yel euh 13g aa*	0.002	1092	29.55	4.72	345	(34)	14336	(34)	9.05
zr nm3 yel euh 12g aa2	0.005	711	18.19	2.02	518	(33)	21839	(33)	9.50

Notes: d, nm represent angles of diamagnetic and paramagnetic susceptibility on a barrier style Frantz separator at 1.4 amps; nm1.0a represent lower amperage paramagnetic splits. Mineral dissolution and chemistry were adapted from methods developed by Krogh (1973), Parrish et al. (1987), and Mattinson (2005). Aliquots of dissolved sample were spiked with a mixed $^{208}Pb/^{235}U$ tracer. The Pb and U samples were loaded onto single rhenium filaments with silica gel and graphite, respectively; isotopic compositions were measured in multicollector, static mode on a VG Sector 54 mass spectrometer at the University of Wyoming, Laramie, with ^{204}Pb in Daly-photomultiplier collector if the $^{206}Pb/^{204}Pb$ value was greater than 200, and all other isotopes in Faraday collectors. Mass discrimination factors of 0.108 to 0.060 ± 0.06 %/amu were determined for Pb based on silica gel batch and replicate analyses of National Institute of Standards and Technology (NIST) SRM 981; U mass discrimination was consistently 0.0 ± 0.06%/amu. Procedural blanks for zircon decreased from 10 pg to less than 5 pg Pb during the course of the study. Uranium blanks were consistently less than 1 pg. Sphene blanks were 20 pg Pb and less than 1 pg U. Concordia coordinates, U-Pb dates, $^{206}Pb/^{204}Pb$ vs. $^{238}U/^{204}Pb$ isochrons, weighted averages, and uncertainties were calculated using PBDAT and ISOPLOT programs (Ludwig 1988, 1991); initial Pb isotopic compositions estimated by the Zartman and Doe (1981) model mantle for 150 Ma. The decay constants used by PBDAT are those recommended by the IUGS Subcommission on Geochronology (Steiger and Jäger, 1977): 0.155125×10^{-9}/yr for ^{238}U, 0.98485×10^{-9}/yr for ^{235}U and present-day $^{238}U/^{235}U$ = 137.88. The $^{208}Pb/^{235}U$ tracer was calibrated against MIT2 gravimetric standard and yielded a $^{206}Pb/^{238}U$ date of 419.26 ± 0.64 Ma for zircon standard R33 ($^{207}Pb/^{235}U$ date of 420.11 ± 0.59 Ma), in good agreement with the ROM date for R33 (Black et al., 2004). The $^{206}Pb/^{238}U$ dates corrected for ^{230}Th disequilibrium used the equations of Schärer (1984). Ratios of Th/U for the minerals are based on radiogenic ^{208}Pb and growth from 150

Corrected atomic ratios (cont.)						Ages# (Ma)					Rho	Rho
$^{206}Pb/^{238}U$	%err	$^{207}Pb/^{235}U$	%err	$^{207}Pb/^{206}Pb$	%err	$^{206}Pb/^{238}U$	abs err	$^{206}Pb^{Th}/^{238}U$	$^{207}Pb/^{235}U$	$^{207}Pb/^{206}Pb$	6/8-7/5‡	a-m††
sph 6/4 vs. 238/4 isochron date)												
0.02345	(0.49)	0.1595	(1.07)	0.0493	(0.80)	149.41	(0.73)	149.48	150.2	163	0.72	0.97
0.02381	(1.02)	0.1603	(3.26)	0.0488	(2.76)	151.71	(1.53)	151.69	151.0	139	0.62	0.71
0.02368	(0.45)	0.1615	(0.73)	0.0495	(0.44)	150.88	(0.67)	150.94	152.0	170	0.83	0.95
0.02369	(0.44)	*no measurement of ^{207}Pb*				150.92	(0.65)	150.98				0.98
weighted average 206/238 date)												
0.02343	(0.84)	0.1666	(3.20)	0.0516	(2.77)	149.28	(1.24)	149.36	156.5	267	0.60	1.00
0.02280	(0.44)	0.1565	(1.59)	0.0498	(1.35)	145.33	(0.64)	145.41	147.6	185	0.63	1.00
0.02298	(0.64)	0.1614	(2.35)	0.0509	(2.04)	146.46	(0.92)	146.54	151.9	238	0.59	1.00
0.02349	(0.44)	0.1607	(1.34)	0.0496	(1.12)	149.66	(0.65)	149.75	151.3	177	0.62	1.00
0.02337	(0.32)	0.1586	(0.45)	0.0492	(0.29)	148.91	(0.47)	148.99	149.5	159	0.78	1.00
0.02344	(0.31)	0.1586	(0.33)	0.0491	(0.09)	149.36	(0.46)	149.45	149.5	152	0.96	1.00
147.43 ± 0.33 Ma (MSWD = 1.42) (5 pt.* sph and zr 6/4 vs. 238/4 isochron date)												
0.02302	(0.32)	0.1559	(0.34)	0.0491	(0.12)	146.72	(0.46)	146.81	147.1	153	0.93	1.00
0.02373	(0.32)	0.1612	(0.40)	0.0493	(0.22)	151.17	(0.47)	151.27	151.7	161	0.83	1.00
0.02321	(0.32)	0.1571	(0.34)	0.0491	(0.11)	147.88	(0.46)	147.97	148.1	152	0.95	1.00
0.02319	(0.31)	0.1572	(0.35)	0.0492	(0.13)	147.77	(0.46)	147.87	148.2	155	0.92	1.00
0.02312	(0.32)	0.1566	(0.32)	0.0491	(0.06)	147.33	(0.46)	147.42	147.8	155	0.98	1.00
0.02276	(0.32)	0.1542	(0.40)	0.0491	(0.23)	145.05	(0.45)	145.14	145.6	154	0.82	1.00
0.02319	(0.32)	0.1571	(0.34)	0.0492	(0.10)	147.76	(0.47)	147.84	148.2	155	0.96	1.00
0.02346	(0.43)	0.1590	(0.76)	0.0491	(0.52)	149.50	(0.64)	149.48	149.8	155	0.75	0.94
0.02333	(0.81)	0.1604	(1.57)	0.0499	(0.97)	148.64	(1.18)	148.70	151.0	189	0.86	0.80
sph and zr weighted average 206/238 date)												
0.02307	(0.32)	0.1580	(0.34)	0.0497	(0.12)	147.04	(0.46)	147.13	148.9	179	0.94	1.00
0.02354	(0.31)	0.1603	(0.38)	0.0494	(0.19)	149.99	(0.47)	150.08	150.9	166	0.87	1.00
0.02326	(0.32)	0.1597	(0.45)	0.0498	(0.28)	148.21	(0.47)	148.30	150.4	186	0.78	1.00
0.02328	(0.35)	0.1595	(0.64)	0.0497	(0.48)	148.33	(0.51)	148.41	150.3	181	0.68	1.00
0.02328	(0.78)	0.1626	(1.96)	0.0507	(1.50)	148.33	(1.15)	148.40	153.0	226	0.72	0.99
0.02316	(0.49)	0.1574	(0.71)	0.0493	(0.38)	147.62	(0.72)	147.68	148.4	162	0.87	0.68
aa & CA zr weighted average 206/238 date)												
0.02312	(0.32)	0.1565	(0.41)	0.0491	(0.24)	147.35	(0.47)	147.44	147.7	153	0.83	1.00
0.02319	(0.33)	0.1574	(0.62)	0.0492	(0.46)	147.80	(0.48)	147.89	148.5	159	0.67	1.00
0.02339	(0.32)	0.1592	(0.55)	0.0494	(0.40)	149.03	(0.48)	149.12	150.0	165	0.70	1.00
0.02322	(0.32)	0.1576	(0.43)	0.0492	(0.26)	147.95	(0.47)	148.04	148.6	159	0.80	1.00
0.02323	(0.34)	0.1576	(0.59)	0.0492	(0.43)	148.05	(0.50)	148.14	148.6	157	0.69	1.00
0.02329	(0.32)	0.1577	(0.40)	0.0491	(0.21)	148.40	(0.47)	148.49	148.7	154	0.85	1.00
0.02325	(0.31)	0.1572	(0.32)	0.0490	(0.06)	148.19	(0.46)	148.28	148.3	150	0.98	1.00
aa zr weighted average 206/238 date)												
0.02229	(0.32)	0.1514	(0.40)	0.0493	(0.21)	142.08	(0.45)	142.17	143.2	161	0.84	1.00
0.02278	(0.39)	0.1562	(1.22)	0.0497	(1.02)	145.21	(0.56)	145.30	147.4	182	0.62	1.00
0.02380	(0.33)	0.1630	(0.49)	0.0497	(0.33)	151.62	(0.49)	151.71	153.3	179	0.75	1.00
0.02310	(0.36)	0.1571	(0.49)	0.0493	(0.30)	147.22	(0.52)	147.31	148.2	163	0.79	1.00
0.02394	(0.32)	0.1700	(0.38)	0.0515	(0.18)	152.50	(0.47)	152.60	159.5	264	0.87	1.00
0.02283	(0.44)	0.1560	(1.15)	0.0496	(0.96)	145.49	(0.63)	145.59	147.2	174	0.60	1.00
0.02292	(0.40)	0.1558	(0.78)	0.0493	(0.60)	146.06	(0.58)	146.15	147.0	163	0.65	1.00

Ma. Abbreviations: aa—air abraded; anh—anhedral; CA—chemically abraded; dk—dark yellow; euh—euhedral; g—number of grains; incl.—with inclusions; lt—pale yellow to colorless; lt br—light brown; mm—shortest diameter in millimeters; MSWD—mean square of weighted deviates; p—pick number; s—single grain; sm—small; sph—sphene; yel—yellow to honey colored; zr—zircon.

*Used in age calculation.

†ComPb: common Pb corrected for laboratory blank of 10 ± 6 pg Pb for zircon and 20 ± 6 pg Pb for sphene analyses. Isotopic composition of blank was 19.09 ± 0.2, 15.652 ± 0.1, 38.81 ± 0.2 for 6/4, 7/4, and 8/4, respectively.

§$^{206}Pb/^{204}Pb$, $^{238}U/^{204}Pb$ corrected for blank and mass discrimination, all others corrected for blank, mass discrimination and initial Pb, using model mantle Pb isotopic values for 150 Ma ($^{206}Pb/^{204}Pb$, $^{207}Pb/^{204}Pb$, $^{208}Pb/^{204}Pb$ =17.80, 15.46, 37.50, respectively; Zartman and Doe, 1981). Values in parentheses are 2σ errors in percent, except for $^{206}Pb/^{238}U$ ages, which are absolute in m.y.

#Ages: $^{206}Pb^{Th}/^{238}U$ date corrected for initial ^{230}Th disequilibria, using estimated $[Th/U]_{magma}$ = 2.85, based on averages of measured Bear Mountain intrusive complex samples. $[Th/U]_{mineral}$ calculated from radiogenic ^{208}Pb and growth from 150 Ma. $\lambda(^{232}Th) = 4.9475 \times 10^{-11}$/yr; $\lambda(^{230}Th) = 9.22 \times 10^{-6}$/yr.

‡Rho 6/8-7/5: $^{206}Pb/^{238}U$ vs. $^{207}Pb/^{235}U$ error correlation coefficient.

§§Rho a-m: $^{206}Pb/^{204}Pb$ vs. $^{238}U/^{204}Pb$ error correlation coefficient.

TABLE 2. VARIATIONS IN $^{206}Pb/^{238}U$ DATES WITH CHOICE OF INITIAL Pb ISOTOPIC COMPOSITION

		Dates (Ma)			
	$^{206}Pb/^{204}Pb$ corrected	$^{206}Pb/^{238}U$ ZD man	abs err	$^{206}Pb/^{238}U$ SK 150	abs err
DP2-20z bio-hbl tonalite					
sphene					
sph nm1.0a lt 0.25mm	153	149.41	(0.73)	148.67	(0.72)
sph nm1.0a dk 0.40mm*	75	151.71	(1.53)	149.93	(1.53)
sph nm1.0a yel 0.25mm p1*	194	150.88	(0.67)	150.31	(0.66)
sph nm1.0a yel 0.25mm p2*	217	150.92	(0.65)	150.41	(0.65)
zircon					
zr d-2 c'less euh 0.05mm*	92	149.28	(1.24)	147.94	(1.17)
zr d-1 yel euh sm 0.03mm	777	145.33	(0.64)	145.20	(0.56)
zr d-1 yel euh lg 7g 0.1mm	131	146.46	(0.92)	145.60	(0.88)
zr d-2 yel euh sm 0.03mm aa*	245	149.66	(0.65)	149.22	(0.61)
zr d-2 yel euh lg 24g 0.2mm aa*	5281	148.91	(0.47)	148.89	(0.47)
zr d-2 yel euh lg 29g 0.15mm CA*	10336	149.36	(0.46)	149.35	(0.46)
DP4-8z hbl-px gabbro					
zr d-1 pk anh sA	2968	146.72	(0.46)	146.69	(0.46)
zr nm1 pk anh sB	2188	151.17	(0.47)	151.13	(0.47)
zr d-1 yel anh sC aa*	508189	147.88	(0.46)	147.88	(0.46)
zr d-1 lt br anh sD aa*	15318	147.77	(0.46)	147.77	(0.46)
zr d-1 yel anh sE aa*	7458	147.33	(0.46)	147.32	(0.46)
zr d-1 yel anh sF aa	6252	145.05	(0.45)	145.04	(0.45)
zr d-1 br anh sG aa*	4673	147.76	(0.47)	147.73	(0.47)
sph nm1.0a dk 0.35mm 11g	219	149.50	(0.64)	149.01	(0.64)
sph nm1.0a lt 0.20mm*	86	148.64	(1.18)	147.20	(1.18)
DP4-10z hbl-px gabbro late pod					
zr nm2 lt br anh sA	35299	147.04	(0.46)	147.04	(0.46)
zr nm2 lt br anh sB	4864	149.99	(0.47)	149.97	(0.46)
zr nm2 lt br anh 8g aa2*	1091	148.21	(0.47)	148.12	(0.47)
zr nm2 lt br anh 24g aa*	380	148.33	(0.51)	148.06	(0.51)
sph nm1.0a yel 0.35mm*	89	148.33	(1.15)	146.94	(1.15)
sph nm1.0a yel 0.35mm p2*	203	147.62	(0.72)	147.08	(0.71)

Notes: $^{206}Pb/^{204}Pb$ corrected for blank and mass discrimination; $^{206}Pb/^{238}U$ dates calculated with initial Pb isotopic values (6/4, 7/4, 8/4) of the Zartman and Doe (1981) mantle (ZD man) at 150 Ma (17.80 ± 0.5, 15.46 ± 0.05, 37.50 ± 0.2) and the Stacey and Kramers (1975) model (SK 150) at 150 Ma (18.474 ± 0.5, 15.618 ± 0.05, 38.356 ± 0.2). Uncertainties for model isotopic values are based on observed ranges for present-day mid-ocean ridge basalt. See Table 1 for other abbreviations.

*Used in age calculation.

affect a few analyses; many of the zircon and titanite analyses are insensitive to the choice of initial Pb isotopic composition, as they have high ratios of radiogenic to common Pb. Correction of $^{206}Pb/^{238}U$ dates for possible Th/U disequilibrium followed Schärer (1984). The disequilibrium corrected dates are used for all $^{206}Pb/^{238}U$ weighted average dates; they overlap in error with the uncorrected values (Table 1).

Biotite-Hornblende Tonalite (DP2-20z)

This sample is part of an intermediate to felsic, composite pluton intruded into the Blue Ridge ultramafic-gabbroic intrusion (Fig. 2). Field relationships indicate that the Blue Ridge intrusion is the earliest stage of the Bear Mountain intrusive complex (Snoke et al., 1981). Because zircon has not been observed in the Blue Ridge intrusion, this composite, crosscutting pluton provides the best means of constraining the age of the host ultramafic-gabbroic intrusion. The older part of the composite pluton is medium-grained, augite-hornblende quartz-bearing diorite with accessory titanite. This phase of the composite pluton contains scarce olivine xenocrysts, presumably derived from the host Blue Ridge intrusion. The dated sample intrudes the quartz-bearing diorite. It is a medium-grained, biotite-hornblende tonalite. Zircon is present as <10-µm inclusions in hornblende, biotite, and plagioclase, and as intergranular crystals as much as 100-µm long. Titanite commonly forms subhedral decorations on hornblende. Some grains show rational faces against adjacent crystals, whereas other grains are ragged, especially against plagioclase. Some late-stage titanite is intergrown with Fe-Ti oxide minerals ± chlorite. The tonalite is chemically similar to other tonalitic plutons in the area (e.g., Pony Peak pluton; Barnes et al., this volume, Chapter 17).

Zircons from this sample appear to be a single morphological population of colorless to pale yellow euhedral grains that are interpreted to be magmatic. There is a wide range in size of the isolated zircon grains, from 350 µm to less than 50 µm in length. Fractions of small and large-sized grains were picked separately to test for any age bias. Zircons appear to be free of cores under visible light. Titanite grains are large (250–400 µm in diameter), euhedral to anhedral grains that range in color from dark to pale yellow. Pale titanite overgrowths occur occasionally on darker cores. Dark titanite commonly indicates a higher temperature growth than pale titanite (e.g., Frost et al., 2001; Aleinikoff et al., 2002). Thus, end-member representatives were selected and analyzed separately to determine whether there was an age progression in titanite growth.

The U-Pb data from titanite and zircon plot in a broad array on a concordia plot (Fig. 3A), with $^{206}Pb/^{238}U$ dates that range from 151.7 to 145.3 Ma (Table 1). There is a general pattern in the ages, with the dark titanite yielding the oldest ages (ca. 152 Ma), pale titanite and abraded (mechanical and chemical) zircon the next oldest (ca. 149.3 Ma), and unabraded zircons the youngest (ca. 149.3–145.3 Ma). The titanite analyses and some of the zircon analyses have $^{206}Pb/^{204}Pb$ of 200 or less. In these cases, the calculated $^{206}Pb/^{238}U$ dates are moderately dependent on the choice of initial Pb isotopic composition (e.g., Verts et al., 1996). For example, the difference in calculated $^{206}Pb/^{238}U$ date between using 150-Ma Zartman and Doe (1981) model mantle values and Stacey and Kramers (1975) model Pb values is ca. 0.5 m.y. for an analysis with a $^{206}Pb/^{204}Pb$ of 200 (Table 2, Fig. 4A). The values in Table 2 and Figure 4A include error propagation of variations in these model isotopic values that approximate the measured variations in MORB. Inclusion of these large variations produces a strong dependence between age uncertainty and measured $^{206}Pb/^{204}Pb$ and a generous estimation of the age uncertainty. The zircon weighted mean date is immobile with this treatment, as it is largely controlled by data with $^{206}Pb/^{204}Pb$ values greater than 200. $^{206}Pb/^{238}U$ dates from yellow titanite are older than the zircon mean date with either reduction. An initial $^{206}Pb/^{204}Pb$ composition that is more radiogenic than the Stacey and Kramers (1975) model could bring the titanite dates into concordance with the zircon date, but it would also produce more scatter in the titanite dates and push the dark titanite date to younger values than the pale population. We favor the Zartman and Doe (1981) model mantle values for the initial Pb isotopic compositions, due to the arc setting of the intrusive complex and the relatively primitive chemical compositions of the Bear Mountain intrusive complex.

A $^{238}U/^{204}Pb$ versus $^{206}Pb/^{204}Pb$ isochron plot avoids this complexity, as no initial Pb correction is needed to plot the analyses. The three yellow to dark titanite analyses yield a good linear fit on a $^{238}U/^{204}Pb$ versus $^{206}Pb/^{204}Pb$ isochron plot (mean square weighted deviation [MSWD] = 0.0514; Fig. 3B). The isochron date of 150.5 ± 0.61 Ma is within error of the weighted, radiogenic $^{206}Pb/^{238}U$ date of these three analyses (150.97 ± 0.44 Ma; Fig. 3A) when reduced with model mantle

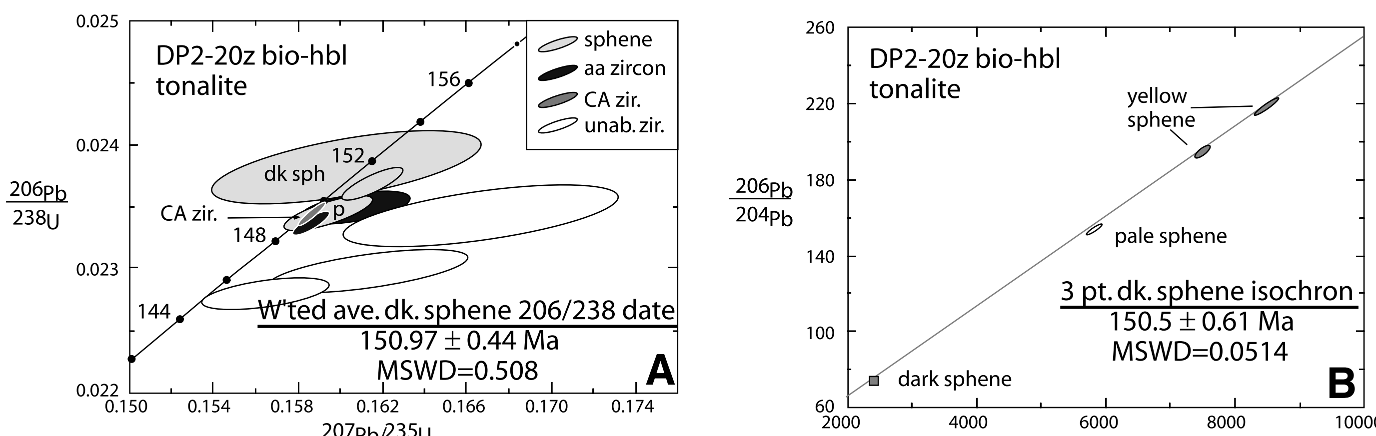

Figure 3. Concordia plot and $^{238}U/^{204}Pb$ vs. $^{206}Pb/^{204}Pb$ isochron plot of data from biotite-hornblende tonalite of the Blue Ridge intrusion (DP2-20z). (A) Data were reduced with model mantle Pb isotopic compositions for 150 Ma (Zartman and Doe, 1981) for the concordia plot. Data from one yellow titanite (sphene) analysis are not shown, as ^{207}Pb was not measured. However, the calculated $^{206}Pb/^{238}U$ date from this analysis is included in the weighted average. Data from dark (dk) and pale (p) titanite fractions are indicated. (B) Data used for the isochron calculation are indicated by filled symbols. The data from the pale titanite do not plot on this isochron and are consistent with microtextural evidence that the pale titanite grew after the darker grains. Agreement between the isochron date of the three dark to yellow titanite analyses (150.5 ± 0.61 Ma) and their weighted radiogenic $^{206}Pb/^{238}U$ date (150.97 ± 0.44 Ma) is interpreted to suggest that 150-Ma model mantle Pb isotopic compositions are appropriate for the initial Pb of these minerals.

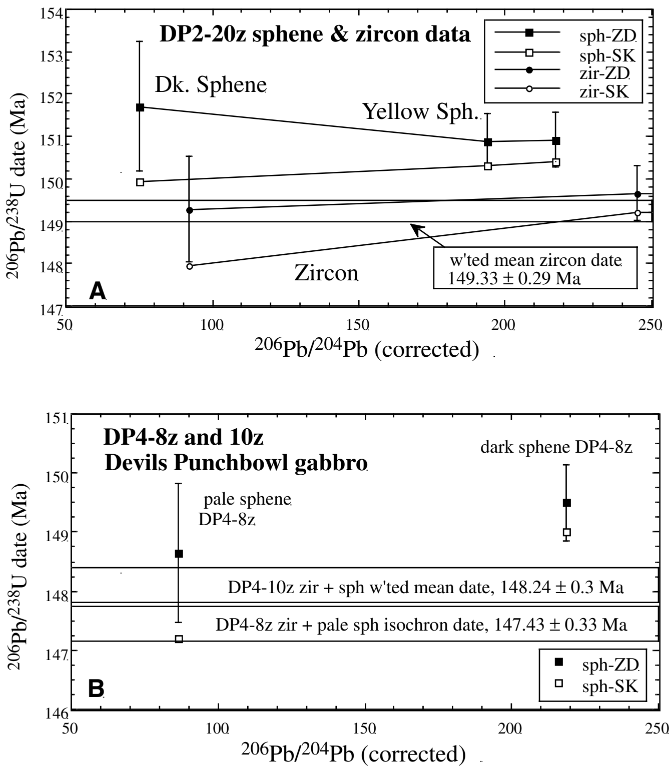

Figure 4. Plots of radiogenic $^{206}Pb/^{238}U$ dates vs. blank-corrected $^{206}Pb/^{204}Pb$ to demonstrate the effect of choice of initial Pb isotopic composition. Data were reduced with 150-Ma values from either the Zartman and Doe (1981; ZD—filled symbols in figure) model mantle ($^{206}Pb/^{204}Pb$ of 17.80 ± 0.5) or Stacey and Kramers (1975; SK—open symbols in figure) crustal model ($^{206}Pb/^{204}Pb$ of 18.474 ± 0.5). The magnitude of the effect of this choice and the size of the age uncertainties both decrease with increasing blank-corrected $^{206}Pb/^{204}Pb$. Uncertainties in model $^{206}Pb/^{204}Pb$ values are estimated to include the range of measurements for modern mid-ocean ridge basalt (Zartman and Doe, 1981). Uncertainties on SK reduced dates are not shown, but are the same magnitudes as for ZD reductions. (A) Dates from yellow titanite (sph) from DP2-20z are older and outside error of the weighted mean age of zircon (zir) analyses for both choices of initial Pb $^{206}Pb/^{204}Pb$. (B) The $^{206}Pb/^{238}U$ date of dark titanite from DP4-8z is outside errors of both Punchbowl zircon dates for the Zartman and Doe (1981) reduction, but overlaps the zircon date of DP4-10z when reduced with Stacey and Kramers (1975) $^{206}Pb/^{204}Pb$ value.

Pb isotopic values for 150 Ma (Zartman and Doe, 1981). This result strengthens our interpretation that model mantle Pb isotopic compositions are appropriate as estimates of initial Pb for these analyses. The pale titanite results do not plot on the isochron from the other three titanite analyses (Fig. 3B) and have a distinctly younger $^{206}Pb/^{238}U$ date (149.4 ± 0.73 Ma; Table 1, Fig. 3A). This result is consistent with the observation of pale overgrowths on darker titanite and suggests to us that either the pluton crystallized slowly as it cooled over a 1- to 2-m.y. period, or a slightly younger magmatic event triggered an additional pulse of titanite growth in this body (see below).

Variation in radiogenic $^{206}Pb/^{208}Pb$ (Table 1) also supports evidence for either a protracted period of titanite growth or multiple events. The dark titanite analysis has the lowest $^{206}Pb/^{208}Pb$ (~0.9), pale titanite has the highest (~3.0), and the yellow titanite analyses are intermediate (~2.5). We interpret these results to indicate that the U/Th composition of the melt evolved by preferential incorporation of Th into accessory phases and that this evolution took 1–2 m.y. in this pluton, based on the ages of the end-member titanites. Variations in U/Th between minerals and parental magma can lead to age biases in young rocks due to deficits or excesses of radiogenic ^{206}Pb (Schärer, 1984). To test for this possibility, we calculated $^{206}Pb/^{238}U$ dates corrected for Th/U disequilibrium (Table 1) by using radiogenic ^{208}Pb as a measure of Th in the minerals and a magma Th/U of 2.85 based on measured compositions from the Bear Mountain intrusive complex (Bushey et al., this volume). The effect of this correction is slight, with changes of only 0.02–0.08 m.y. for the titanite dates (Table 1), and it fails to narrow the age differences between dark titanite, pale titanite, and zircon over a wide range of magmatic Th/U values (Fig. 5).

We interpret the $^{238}U/^{204}Pb$ versus $^{206}Pb/^{204}Pb$ isochron date of 150.5 ± 0.61 Ma from dark and yellow titanite as the best estimate for the age of initial crystallization of this pluton. On this basis, the zircon data either reflect slightly later crystallization in the pluton (149.3 ± 0.3 Ma) or some degree of Pb loss (0.6–3.5%) despite rigorous air abrasion of grains for two of the analyses and chemical abrasion for another. Calculated zircon saturation temperature (Watson and Harrison, 1983) for this sample is 842 °C, based on chemical compositions reported in Bushey et al. (this volume). This temperature is consistent with relatively late zircon crystallization in a dry, tonalitic cumulate. It is also possible that the dark titanite grew in the earlier quartz-bearing dioritic magma. If so, then the dark titanite could represent xenocrystic material from the older host rock. In this case, however, the dark titanite would have had to retain its older U-Pb date for several 100 k.y. as the later magma evolved to tonalite and precipitated zircon and pale titanite. Closure temperatures of at least 700 °C have been reported for titanite in metamorphic settings (Scott and St-Onge, 1995).

Pyroxene-Hornblende Gabbro, Punchbowl Unit (DP4-8z and DP4-10z)

This unit is part of a large, composite pluton that is exposed over ~40 km^2. It consists of pyroxene-hornblende gabbro that locally grades into anorthositic gabbro as well as biotite-hornblende (quartz-bearing) diorite (Snoke et al., 1981; Bushey et al., this volume). Modal proportions vary considerably, even at the outcrop scale. Most samples have major and trace element compositions suggestive of accumulation from a high-Al basaltic magma (Bushey et al., this volume; Barnes et al., this volume, Chapter 17). Two samples were collected for geochronology: a coarse-grained, slightly pegmatitic sample with hornblende, plagioclase, biotite, and minor quartz (DP4-8z) and a late-stage,

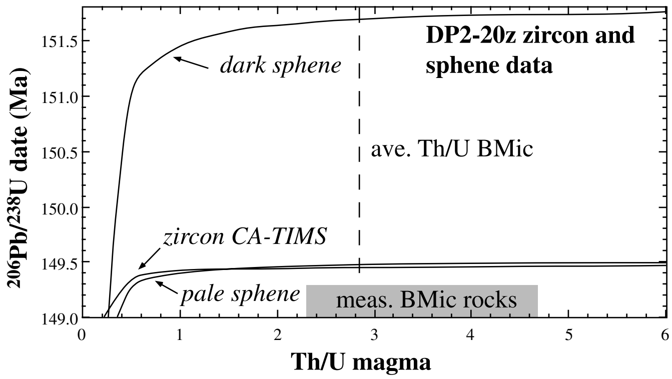

Figure 5. Plot of $^{206}Pb/^{238}U$ mineral dates from DP2-20z corrected for Th/U disequilibrium for a range of magma Th/U values. Dark titanite (sphene) and chemical abrasion thermal ionization mass spectrometry zircon analyses have the most variation in Th/U of any samples (indicated by radiogenic $^{206}Pb/^{208}Pb$ values of 0.94 and 6.97 respectively). Extreme Th/U magma values of <0.4 are required to bring the dates of these two minerals into concordance. Measured Th/U of representative rocks of the Bear Mountain intrusive complex (BMic) range from 2.29 to 4.72 and average 2.85 (Bushey et al., this volume).

magmatic pod (DP4-10z) with distinctive, concentric layers of plagioclase and hornblende, weakly developed harrisitic texture, and a coarse-grained interior (3-cm crystals; Fig. 6). The hornblende is prismatic, with interstitial to poikilitic plagioclase (~An_{60}). Accessory phases are Fe-Ti oxides, interstitial alkali feldspar, and subhedral to anhedral titanite up to 1.5 mm in length. Ragged fractures in the hornblende show replacement by epidote ± fine-grained titanite ± chlorite, and the plagioclase shows deformation that ranges from bent crystals to subgrain development. This pod crosscuts magmatic foliation in the

Figure 6. Photograph of late-stage magmatic pod (DP4-10z) from the Punchbowl unit. Note lens cap for scale. Concentric layers of plagioclase (beneath lens cap) and hornblende surround coarse-grained interior composed of 3-cm length crystals.

pyroxene-hornblende gabbro and is interpreted as a pocket of late, H_2O-rich liquid in the crystallizing pluton. Both samples yielded zircon and titanite. Zircon from both samples are large (~750 × 450 µm, typically) and anhedral. The titanite from DP4-8z ranges in color from dark and reddish to pale yellow, although no core-rim relationships were detected. The titanite from DP4-10z is more uniformly honey colored.

The zircon data from DP4-8z, the texturally earlier sample of the Punchbowl unit, display a range in $^{206}Pb/^{238}U$ dates from 151.2 to 145.1 Ma (Table 1, Fig. 7A). All of these analyses are from single grains, and five of the seven were air abraded. Four of the analyses of air-abraded zircon plot in a tight cluster with overlapping $^{206}Pb/^{238}U$ dates and indicate a weighted average of 147.7 ± 0.23 Ma. Analyses of dark titanite and one single zircon have older $^{206}Pb/^{238}U$ dates, ca. 149.5 and ca. 151 Ma, respectively. We interpret the date from the older zircon to reflect slight inheritance, because it is so much older than those from all the other analyses. The two zircon analyses that are younger than the cluster of four are interpreted to reflect Pb loss. The $^{206}Pb/^{238}U$ date from the cluster of four zircons is interpreted as the crystallization age of zircon in this sample, although it is possible that there is some Pb loss even in these analyses. However, the data from the pale titanite analysis lie on a linear regression of these four zircon analyses on a $^{238}U/^{204}Pb$ versus $^{206}Pb/^{204}Pb$ isochron plot (Fig. 7C). Including the titanite data yields an isochron date of 147.43 ± 0.33 Ma with a good linear fit (MSWD = 1.42). This date is indistinguishable from the weighted average $^{206}Pb/^{238}U$ date of the zircon alone and is interpreted to indicate that the pale titanite grew at the same time as these zircon grains. The data from dark titanite is off the linear regression of the pale titanite and zircon analyses (Fig. 7C) and has a $^{206}Pb/^{238}U$ date that is nearly 2 m.y. older (149.5 ± 0.64 Ma). The radiogenic $^{206}Pb/^{208}Pb$ for the two titanite analyses are distinct as well (0.9 versus 2.6) and support our interpretation that titanite grew over a 2-m.y. period. The pattern of mineral dates is very similar in this sample to the pattern in DP2-20z discussed above, and we interpret them to record a progression of crystallization of the pluton. Initial crystallization occurred at 149.5 ± 0.64 Ma, based on data from dark titanite, and was followed 1–2 m.y. later by crystallization of zircon and pale titanite.

The U-Pb data from DP4-10z, the late magmatic pod in the Punchbowl unit, is slightly less complicated, because there is only one morphology of titanite, and the data from two titanite analyses are internally consistent. Titanite data yield a weighted $^{206}Pb/^{238}U$ date of 147.9 ± 0.6 Ma and have similar radiogenic $^{206}Pb/^{208}Pb$ values of ~3.02–2.78 (Table 1). Data from two fractions of small, air-abraded zircons overlap this date and produce a four-point, titanite and zircon, $^{206}Pb/^{238}U$-weighted date of 148.24 ± 0.30 Ma (MSWD = 0.94; Fig. 7B, Table 1). A linear regression of these same four data points on a $^{238}U/^{204}Pb$ versus $^{206}Pb/^{204}Pb$ isochron plot yields nearly the same result, 148.12 ± 0.41 Ma, with a good linear fit (MSWD = 1.49; Fig. 7D). Data from two large, single zircon grains yield both older and younger $^{206}Pb/^{238}U$ dates compared to this cluster (ca. 150

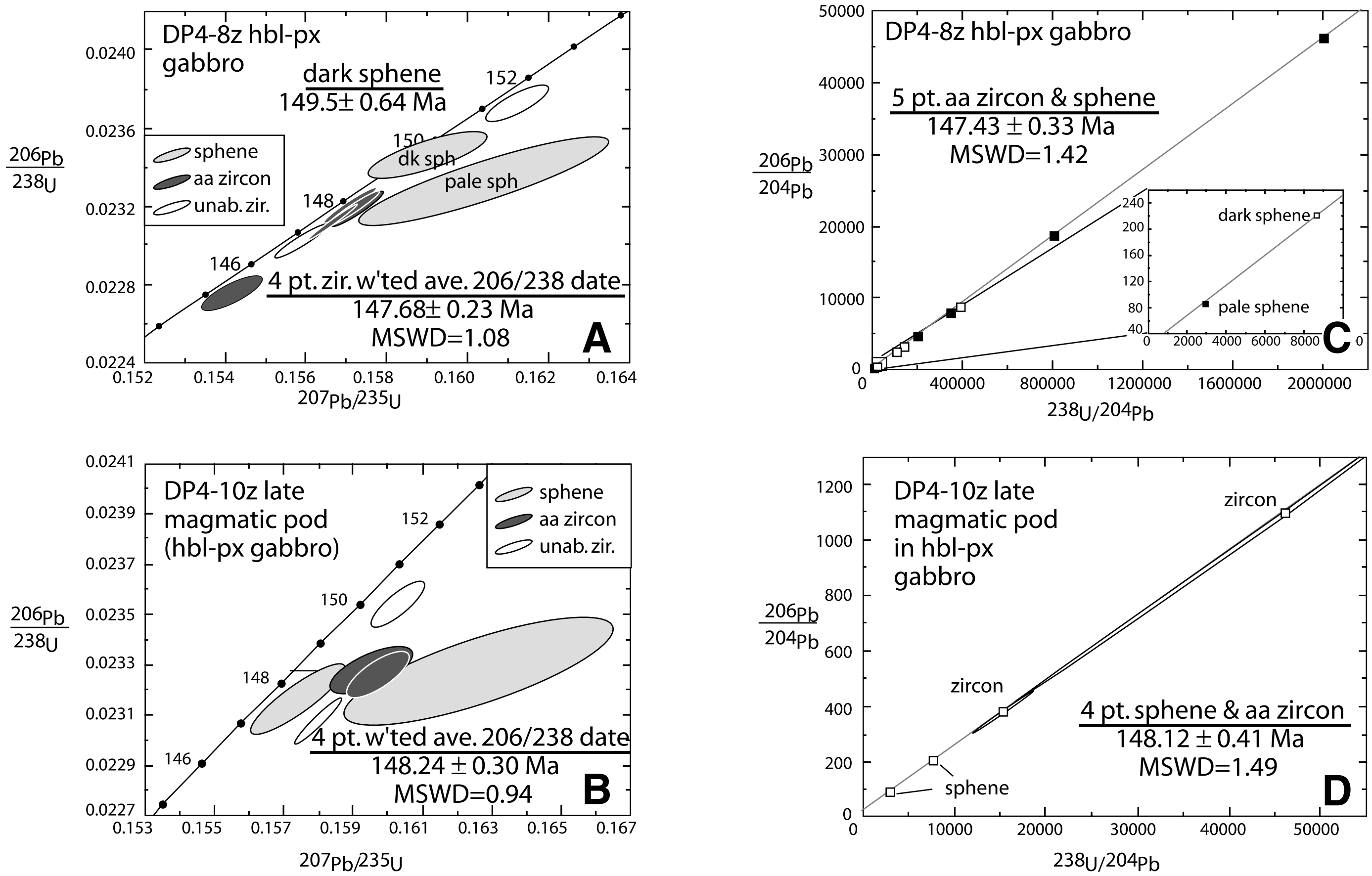

Figure 7. (A, B) Concordia plots and (C, D) $^{238}U/^{204}Pb$ vs. $^{206}Pb/^{204}Pb$ isochron plots of data from two samples of the Punchbowl unit. DP4-8z is from a coarse-grained, pyroxene-hornblende gabbro that is fairly typical of the intrusion. DP4-10z is from a distinct, late-stage magmatic pod, shown in Figure 6. Isochron date from four air-abraded zircon fractions and pale titanite data from DP4-8z (147.43 ± 0.33 Ma; filled symbols in C) agrees with the radiogenic $^{206}Pb/^{238}U$ date of the four air-abraded zircon fractions alone (147.68 ± 0.23 Ma in A) and is interpreted to indicate that pale titanite grew at the same time as zircon in this sample. Data from dark titanite plot above this isochron and reduce to an older radiogenic $^{206}Pb/^{238}U$ date of 149.5 ± 0.64 Ma. The late, magmatic pod (DP4-10z) yielded only one morphology of titanite. Zircon and titanite grew at the same time in this sample (148.24 ± 0.30 Ma), slightly earlier than the growth of pale titanite and zircon in DP4-8z. Taken together, these data document 1–2 m.y. of crystallization in the Punchbowl unit, either due to multiple pulses of magma injection or protracted crystallization. Both samples also contain evidence for slight inheritance of zircon that is at least 151 Ma in age.

and ca. 147 Ma, respectively; Table 1) and are interpreted to reflect slight inheritance and Pb loss. Our best estimate for the timing of crystallization of this late magmatic pod comes from the weighted average $^{206}Pb/^{238}U$ date of the two titanite and two air-abraded zircon analyses, 148.24 ± 0.30 Ma. This date is barely within error to slightly older than the date of crystallization of pale titanite and zircon from the texturally earlier Punchbowl sample, DP4-8z, and 1–2-m.y. later than the dark titanite date from that sample (Fig. 4B). The $^{206}Pb/^{238}U$ dates of titanite from DP4-8z and DP4-10z are somewhat dependent on choice of initial Pb isotopic composition (Table 2, Fig. 4B), but we interpret the agreement between the $^{238}U/^{204}Pb$ versus $^{206}Pb/^{204}Pb$ isochron dates and the radiogenic $^{206}Pb/^{238}U$ dates to support our choice of the Zartman and Doe (1981) mantle value for initial $^{206}Pb/^{204}Pb$. The model $^{207}Pb/^{204}Pb$ values may not be appropriate, however, as both zircon and titanite data from DP4-8z and DP4-10z are slightly discordant, and the degree of discordance increases with proportion of common Pb (inverse of $^{206}Pb/^{204}Pb$). A different choice of initial $^{207}Pb/^{204}Pb$ could bring all these values into concordance.

Taken together, the data from these two samples of the Punchbowl unit are interpreted to record a protracted period of crystallization. Dark titanite commonly has higher Fe and Al content (e.g., Aleinikoff et al., 2002) and grows at higher temperatures than pale titanite (Frost et al., 2001). The $^{206}Pb/^{238}U$ date of the dark titanite from DP4-8z is the earliest date (149.5 ± 0.6 Ma) and is interpreted to record the initial stages of crystallization of the pluton. Pale titanite and zircon from both samples record crystallization 1–2 m.y. after the dark titanite and document continued crystallization of an evolving magma, perhaps at lower temperatures. Calculated zircon saturation temperatures for these samples are ~640–650 °C (Watson and Harrison, 1983; Bushey et al., this volume), reflecting the cumulate nature of this unit and near-solidus crystallization of zircon.

Biotite–Two-Pyroxene Quartz-Bearing Diorite, Buck Lake Unit (DP1-13z)

This is a medium- to coarse-grained plutonic unit with tabular plagioclase, ortho- and clinopyroxene, and oikocrystic biotite. The analyzed sample contains scarce alkali feldspar, but other samples from the outcrop have poikilitic alkali feldspar and are monzodioritic. The Buck Lake unit is distinct from the Punchbowl unit in the relative abundance of alkali feldspar and paucity of primary hornblende (Snoke et al., 1981; Bushey et al., this volume). Field relationships between the Buck Lake and Punchbowl unit have been interpreted to suggest synchronicity (Snoke et al., 1981; Bushey et al., this volume). Zircon grains are euhedral, prismatic, 100 × 250 µm, and honey colored. No titanite was recovered from this sample. The U-Pb data from seven multigrain analyses plot in a relatively tight cluster with $^{206}Pb/^{238}U$ dates that range from 149.1 ± 0.5 to 147.4 ± 0.5 Ma (Fig. 8). The spread in dates is interpreted to reflect a combination of inheritance and Pb loss. Our best estimate for the crystallization age of the unit comes from the weighted $^{206}Pb/^{238}U$ date of four air-abraded zircon fractions and one chemically abraded fraction: 148.2 ± 0.2 Ma (Fig. 8, Table 1). This date is within error of the last stages of crystallization of the Punchbowl unit and 2–3 m.y. later than the initial crystallization date of the tonalite (DP2-20z). Saleeby et al. (1982) reported a date of 153 ± 2 Ma for the monzodiorite unit based on a single 10-mg fraction of zircon. Their analysis had a relatively low $^{206}Pb/^{204}Pb$ of 700, and the absolute date is relatively sensitive to choice of initial Pb isotopic composition. The $^{206}Pb/^{204}Pb$ ratios of our data are significantly higher (1400–20,000), and the calculated dates are less sensitive to choice of initial isotopic composition. It is also possible that the Saleeby et al. (1982) analysis included a significant inherited component, as there is evidence for the presence of inheritance in our data, and they dissolved about one-hundred times as many grains for their analysis as we did.

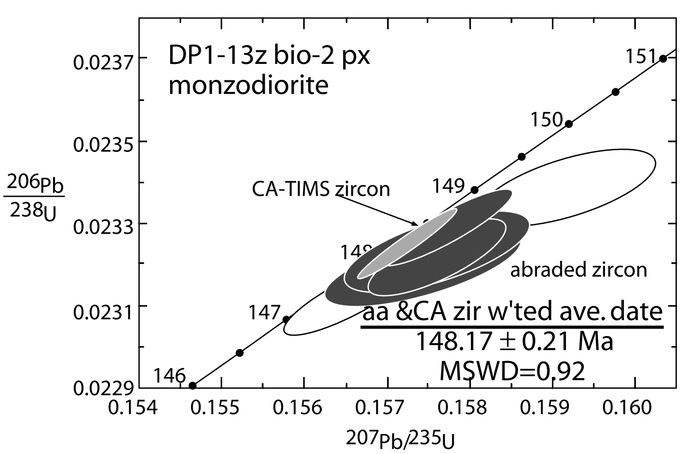

Figure 8. Concordia plot of zircon U-Pb data from biotite–two-pyroxene (bio-2 px) monzodiorite of Buck Lake unit (DP1-13z). Data from air-abraded grains (aa; black-filled ellipses) and annealed and chemically abraded grains (chemical abrasion thermal ionization mass spectrometry; gray-filled ellipse) have a weighted mean $^{206}Pb/^{238}U$ date, 148.17 ± 0.21 Ma, within error of the date of the Punchbowl unit.

Late Mafic Dike (DP1-35z)

This sample is from a quartz-bearing pod in a 2-m-thick, medium- to fine-grained, hornblende quartz diorite dike. The dike crosscuts foliation in the inner aureole of the Bear Mountain intrusive complex, lacks penetrative deformation, and its age thus places a lower limit on the timing of magmatism of the intrusive complex. The sample is an unusual 0.25-m-diameter portion of the dike, with visible free quartz, ~3 mm in size, and a matrix that is finer than the rest of the dike. The pod can be due to either late-stage differentiation or partial digestion of a country rock. We prefer the former interpretation, because quartz is intergrown with all of the primary phases in the sample. The zircons are relatively small (~150 µm or less in length), euhedral, yellow grains. Visible inclusions exist in many of the grains. The U-Pb data from seven multigrain fractions show the widest dispersion of any of the samples in this study, with $^{206}Pb/^{238}U$ dates from ca. 153 to 142 Ma. We interpret the data to imply that most of the zircon grew during crystallization of the dike and is not derived from significantly older country rock. Data from one fraction of inclusion-rich grains that were strongly air-abraded are distinctly discordant and have a $^{207}Pb/^{206}Pb$ age of 264 Ma. These results establish that inherited zircon components exist and that they are at least 260 Ma and may be as old as Paleoproterozoic (Fig. 9). Our best estimate of the crystallization age of the zircon comes from the weighted $^{206}Pb/^{238}U$ average date from two fractions of air-abraded zircon (145.4 ± 0.4 Ma; Fig. 9). Data from three other analyses are interpreted to reflect some inherited components, and one fraction of unabraded grains displays Pb loss. The date of ca. 145 Ma is clearly later than that for all other samples (Fig. 10), consistent with the field relationships, and establishes a maximum duration of magmatism in the Bear Mountain complex of 4–6 m.y. Moreover, this age is similar to U-Pb ages determined for the nearby Bear Peak and Pony Peak plutons (Allen and Barnes, this volume).

DISCUSSION

The new geochronological data presented in this chapter are complex and fairly difficult to interpret as precise crystallization ages, because each sample produced a 3- to 10-m.y. range of dates. The spread in dates reflects minor inheritance and Pb loss, but also adds insight into duration of crystallization processes. Even in the most conservative interpretation, the data establish that the Bear Mountain intrusive complex was emplaced be-

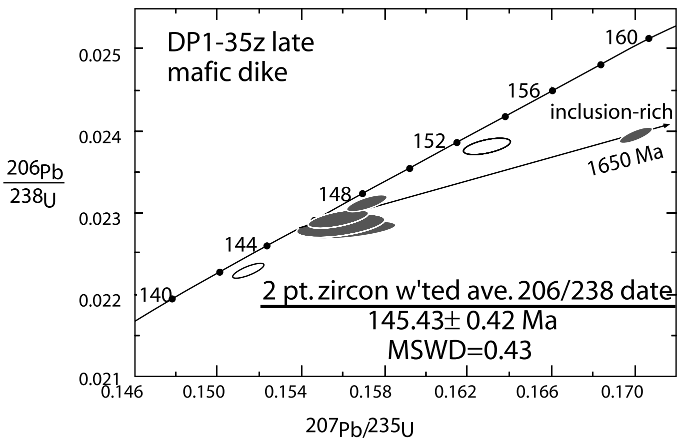

Figure 9. Concordia plot of zircon U-Pb data from late mafic dike, DP1–35z. Data from air-abraded, inclusion-rich grains yield strong evidence for inherited components, at least as old as 264 Ma ($^{207}Pb/^{206}Pb$ date) and possibly Paleoproterozoic. The weighted mean $^{206}Pb/^{238}U$ date, 145.43 ± 0.42 Ma, of two analyses of inclusion-free, air-abraded grains is distinctly later than the dates of the other samples analyzed.

tween ca. 151 and 147 Ma, with a minimum duration of 1.5 m.y. (Fig. 10). If the late mafic dike is considered to be part of the complex, then the duration of magmatism could have been as much as 6 m.y. The new data also support the relative chronology determined from field relationships, although they clearly argue against using petrographic characteristics as indicative of a general age progression during magma genesis. For example, leucocratic rocks commonly intrude the mafic rocks of the Bear Mountain intrusive complex. The sample of biotite-hornblende tonalite (DP2-20z) that yielded the oldest ages in this new geochronological study is from a satellitic, composite pluton that intrudes the Blue Ridge ultramafic-gabbroic intrusion. The absolute age of this leucocratic rock, however, is older than dated samples from either the Punchbowl or Buck Lake plutonic units.

The age pattern from old, dark titanite to younger, pale titanite and zircon in the Blue Ridge and Punchbowl samples has intriguing implications for crystallization processes and mineral isotopic systematics. One possible interpretation of this pattern is that the dark titanite grains are xenocrystic and inherited from an earlier body. We are not aware of a previously documented occurrence of inherited titanite in magmatic rocks, so this could be the first recorded instance of the phenomenon. This interpretation would also imply U-Pb closure temperatures in titanite that are higher than generally accepted (600–700 °C; e.g., Frost et al., 2001; Aleinikoff et al., 2002) for the older age to survive during generation of the new pluton. An alternative interpretation of the age pattern for titanite and zircon is that the data have captured a crystallization history of 1.5–2 m.y. in each pluton. The tonalite intruded into the Blue Ridge intrusion (DP2-20z) is a differentiate in the core of a composite pluton (Fig. 2), so it is conceivable that cooling and crystallization was relatively slow (1–2 m.y.). The Punchbowl unit is a complex body produced by multiple intrusive sheets (hundreds to thousands of them), so a model of protracted crystallization in this body is certainly possible. It is important to note, however, that the Punchbowl unit exhibits more or less uniform magmatic foliation, and there must have been sufficient interstitial melt to permit communication of strain throughout the composite pluton as it cooled. We envision that later pulses of magmatism either slowed the cooling and crystallization process by injecting additional heat, or actually spurred pulses of crystal growth through renewed fluids and heat. A combination of these processes is also possible. At this stage, we favor the protracted crystallization interpretation, although we cannot completely rule out xenocrystic titanite.

Coleman et al. (2004) and Glazner et al. (2004) invoked incremental assembly by successive sheets to explain the nearly 4-m.y. range of zircon dates for the Half Dome granodiorite of the Tuolumne intrusive suite. Our data from the Bear Mountain intrusive complex differ from their results in that we have documented protracted crystallization histories (1–2 m.y.) within single samples. The zircon dates from the Half Dome granodiorite young toward the center (Coleman et al. 2004), consistent with protracted crystallization, although the authors do not favor this interpretation. Both studies demonstrate that simple thermal models of cooling and crystallization may be too simplistic, and that detailed, high-precision geochronology in plutonic complexes can elucidate fine-scale features of crystallization.

The new dates on the Bear Mountain intrusive complex place constraints on the timing of deformation in the region. The South Siskiyou Fork fault (Snoke, 1977; Snoke et al., 1981; Fig. 2) is truncated by the Punchbowl unit of the Bear Mountain intrusive complex and thereby predates 149.5 ± 0.6 Ma. This northwest–southeast-striking, high-angle fault is interpreted as a tear fault associated with the Preston Peak (thrust) fault (Snoke, 1977), a local equivalent of the regional Orleans fault system. Upper Jurassic Galice Formation is part of the footwall block of the Orleans fault and contains ca. 153-Ma detrital zircon grains (Miller et al., 2003). Thus, the South Siskiyou Fork fault must have formed between 153 and 149 Ma. This rela-

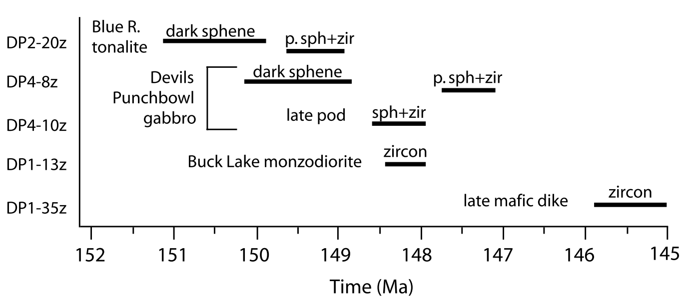

Figure 10. Summary plot of mineral dates from Bear Mountain intrusive complex samples in this study. Abbreviations: p. sph—pale sphene; R.—Ridge; zir—zircon.

tionship indicates that the Bear Mountain intrusive complex was emplaced subsequent to the development of the Orleans (Preston Peak) fault and that the emplacement of the intrusive complex post-dated regional thrust faulting associated with the Late Jurassic Nevadan orogeny (Snoke and Barnes, this volume).

Combining our results with new dates on other plutons in the western Klamath Mountains (e.g., Allen and Barnes, this volume) suggests that the Bear Mountain intrusive complex is part of a long-lived magmatic (arc) pulse that began as early as ca. 151 Ma, probably during Nevadan-age thrusting, and extended at least to ca. 144 Ma (e.g., age of the Pony Peak pluton). In fact, magmatism in the Klamath Mountains continued, with no younger thrusting events, until ca. 136 Ma. However, there seems to be a distinctive set of mainly dioritic plutons that crop out in the western Klamath Mountains that intrude either the Galice Formation (of the western Klamath terrane) or Rattlesnake Creek terrane. Every one of these plutons that has been dated has an age between 150 and 144 Ma (Irwin and Wooden, 1999; Allen and Barnes, this volume). In addition, the Bear Mountain intrusive complex and other "western Klamath" plutons share a number of geochemical similarities, which supports the idea that they are part of a distinct episode of arc magmatism (Barnes et al., this volume, Chapter 17).

CONCLUSIONS

The U-Pb data from titanite and zircon have established that the Bear Mountain intrusive complex was emplaced between 151 and 147 Ma, after the Late Jurassic Nevadan orogeny. Emplacement and crystallization of the complex took at least 1.5 m.y. and may have lasted 6 m.y. Based on age ranges of titanite and zircon, crystallization of individual plutons may have taken 1.5–2 m.y. The timing of deformation of the South Siskiyou Fork fault, an oblique-slip tear fault associated with the Preston Peak (thrust) fault (Orleans fault system), is constrained to the period from ca. 153 to 149 Ma. The Bear Mountain intrusive complex is part of long-lived pulse of arc magmatism that lasted from 151 Ma to at least 144 Ma.

ACKNOWLEDGMENTS

This research was funded by National Science Foundation grants EAR-9902807 to AWS and EAR-9902912 to CGB. Jessica Anderson, Diana Strickland, and Peter Valley assisted with sample preparation and mass spectrometry. We thank Mark D. Schmitz and James M. Mattinson for their thorough and helpful reviews.

REFERENCES CITED

Aleinikoff, J.N., Wintsch, R.P., Fanning, C.M., and Dorais, M.J., 2002, U-Pb geochronology of zircon and polygenetic titanite from the Glastonbury Complex, Connecticut, USA: An integrated SEM, EMPA, TIMS, and SHRIMP study: Chemical Geology, v. 188, p. 125–147, doi: 10.1016/S0009-2541(02)00076-1.

Allen, C.M., and Barnes, C.G., 2006, this volume, Ages and some cryptic sources of Mesozoic plutonic rocks in the Klamath Mountains, California and Oregon, *in* Snoke, A.W., and Barnes, C.G., eds., Geological studies in the Klamath Mountains province, California and Oregon: A volume in honor of William P. Irwin: Boulder, Colorado, Geological Society of America Special Paper 410, doi: 10.1130/2006.2410(11).

Barnes, C.G., Snoke, A.W., Harper, G.D., Frost, C.D., McFadden, R.R., Bushey, J.C., and Barnes, M.A.W., 2006, this volume (Chapter 17), Arc plutonism following regional thrusting: Petrology and geochemistry of syn- and post-Nevadan plutons in the Siskiyou Mountains, Klamath Mountains province, California, *in* Snoke, A.W., and Barnes, C.G., eds., Geological studies in the Klamath Mountains province, California and Oregon: A volume in honor of William P. Irwin: Boulder, Colorado, Geological Society of America Special Paper 410, doi: 10.1130/2006.2410(17).

Black, L.P., Kamo, S.L., Allen, C.M., Davis, D.W., Aleinikoff, J.N., Valley, J.W., Mundil, R., Campbell, I.H., Korsch, R.J., Williams, I.S., and Foudoulis, C., 2004, Improved $^{206}Pb/^{238}U$ microprobe geochronology by the monitoring of a trace-element-related matrix effect; SHRIMP, ID-TIMS, ELA-ICP-MS and oxygen isotope documentation for a series of zircon standards: Chemical Geology, v. 205, p. 115–140, doi: 10.1016/j.chemgeo.2004.01.003.

Blackwelder, E., 1914, A summary of the orogenic epochs in the geologic history of North America: Journal of Geology, v. 22, p. 633–654.

Blake, M.C., Jr., 1984, Tectonostratigraphic terranes in southwestern Oregon, *in* Nilsen, T.H., ed., Geology of the Upper Cretaceous Hornbrook Formation, Oregon and California: Los Angeles, Pacific Section, Society of Economic Paleontologists and Mineralogists, p. 159–165.

Blake, M.C., Jr., Engebretson, D.C., Jayko, A.S., and Jones, D.L., 1985, Tectonostratigraphic terranes in southwest Oregon, *in* Howell, D.G., ed., Tectonostratigraphic terranes of the Circum-Pacific region: Houston, Circum-Pacific Council for Energy and Mineral Resources, Earth Sciences Series 1, p. 147–157.

Bushey, J.C., Snoke, A.W., Barnes, C.G., and Frost, C.D., 2006, this volume, Geology of the Bear Mountain intrusive complex, Klamath Mountains, California, *in* Snoke, A.W., and Barnes, C.G., eds., Geological studies in the Klamath Mountains province, California and Oregon: A volume in honor of William P. Irwin: Boulder, Colorado, Geological Society of America Special Paper 410, doi: 10.1130/2006.2410(14).

Coleman, D.S., Gray, W., and Glazner, A.F., 2004, Rethinking the emplacement and evolution of zoned plutons: Geochronologic evidence for incremental assembly of the Tuolumne intrusive suite, California: Geology, v. 32, p. 433–436, doi: 10.1130/G20220.1.

Davis, G.A., Monger, J.W.H., and Burchfiel, B.C., 1978, Mesozoic construction of the Cordilleran "collage," central British Columbia to central California, *in* Howell, D.G., and McDougall, K.A., eds., Mesozoic paleogeography of the western United States, Pacific Coast Paleogeography II: Los Angeles, Pacific Section, Society of Economic Paleontologists and Mineralogists, p. 1–32.

Frost, B.R., Chamberlain, K.R., and Schumacher, J., 2001, Sphene (titanite): Phase relations and role as a geochronometer: Chemical Geology, v. 172, p. 131–148, doi: 10.1016/S0009-2541(00)00240-0.

Glazner, A.F., Bartley, J.M., Coleman, D.S., Gray, W., and Taylor, R.Z., 2004, Are plutons assembled over millions of years by amalgamation from small magma chambers? GSA Today, v. 14, no. 4/5, p. 4–11, doi: 10.1130/1052-5173(2004)014<0004:APAOMO>2.0.CO;2.

Gray, G.G., 2006, this volume, Structural and tectonic evolution of the western Jurassic belt along the Klamath River corridor, Klamath Mountains, California, *in* Snoke, A.W., and Barnes, C.G., eds., Geological studies in the Klamath Mountains province, California and Oregon: A volume in honor of William P. Irwin: Boulder, Colorado, Geological Society of America Special Paper 410, doi: 10.1130/2006.2410(07).

Harper, G.D., and Wright, J.E., 1984, Middle to Late Jurassic tectonic evolution of the Klamath Mountains, California-Oregon: Tectonics, v. 3, p. 759–772.

Harper, G.D., Saleeby, J.B., and Heizler, M., 1994, Formation and emplacement of the Josephine ophiolite and the Nevadan orogeny in the Klamath Mountains, California-Oregon: U/Pb zircon and $^{40}Ar/^{39}Ar$ geochronology: Journal of Geophysical Research, v. 99, p. 4293–4321, doi: 10.1029/93JB02061.

Hershey, O.H., 1906, Some western Klamath stratigraphy: American Journal of Science, 4th series, v. 21, p. 58–66.

Hershey, O.H., 1911, Del Norte County [California] geology: Mining and Scientific Press, v. 102, p. 468.

Howell, D.G., Jones, D.L., and Schermer, E.L., 1985, Tectonostratigraphic terranes of the Circum-Pacific region, *in* Howell, D.G., ed., Tectonostratigraphic terranes of the Circum-Pacific region: Houston, Circum-Pacific Council for Energy and Mineral Resources, Earth Sciences Series 1, p. 3–30.

Imlay, R.W., 1959, Succession and speciation of the pelecypod *Aucella:* Washington, D.C., U.S. Geological Survey Professional Paper 314-G, p. 155–169, plates 16–19.

Irwin, W.P., 1972, Terranes of the western Paleozoic and Triassic belt in the southern Klamath Mountains, California: Washington, D.C., U.S. Geological Survey Professional Paper 800-C, p. C103–C111.

Irwin, W.P., 1981, Tectonic accretion of the Klamath Mountains, *in* Ernst, W.G., ed., The geotectonic development of California—Rubey volume 1: Englewood Cliffs, New Jersey, Prentice-Hall, p. 29–70.

Irwin, W.P., 1985, Age and tectonics of plutonic belts in accreted terranes of the Klamath Mountains, California and Oregon, *in* Howell, D.G., ed., Tectonostratigraphic terranes of the circum-Pacific region: Houston, Circum-Pacific Council for Energy and Mineral Resources, Earth Sciences Series 1, p. 187–199.

Irwin, W.P., 1994, Geologic map of the Klamath Mountains, California: Reston, Virginia, U.S. Geological Survey Miscellaneous Investigations Series Map I–2148, scale 1:500,000, 2 sheets.

Irwin, W.P., and Wooden, J.L., 1999, Plutons and accretionary episodes of the Klamath Mountains, California and Oregon: Reston, Virginia, U.S. Geological Survey Open-File Report 99-374, 1 sheet.

Jachens, R.C., Barnes, C.G., and Donato, M.M., 1986, Subsurface configuration of the Orleans fault: Implications for deformation in the western Klamath Mountains, California: Geological Society of America Bulletin, v. 97, p. 388–395, doi: 10.1130/0016-7606(1986)97<388:SCOTOF>2.0.CO;2.

Krogh, T.E., 1973, A low-contamination method for hydrothermal decomposition of zircon and extraction of U and Pb for isotopic age determinations: Geochimica et Cosmochimica Acta, v. 37, p. 485–494, doi: 10.1016/0016-7037(73)90213-5.

Lanphere, M.A., Irwin, W.P., and Hotz, P.E., 1968, Isotopic age of the Nevadan orogeny and older plutonic and metamorphic events in the Klamath Mountains, California: Geological Society of America Bulletin, v. 79, p. 1027–1052.

Ludwig, K.R., 1988, PBDAT for MS-DOS, a computer program for IBM-PC compatibles for processing raw Pb-U-Th isotope data, version 1.24: Reston, Virginia, U.S. Geological Survey Open-File Report 88-542, 32 p.

Ludwig, K.R., 1991, ISOPLOT for MS-DOS, a plotting and regression program for radiogenic-isotope data, for IBM-PC compatible computers, version 2.75: Reston, Virginia, U.S. Geological Survey Open-File Report 91-445, 45 p.

Mattinson, J.M., 2005, Zircon U-Pb chemical abrasion ("CA-TIMS") method: Combined annealing and multi-step partial dissolution analysis for improved precision and accuracy of zircon ages: Chemical Geology, v. 220, p. 47–66, doi: 10.1016/j.chemgeo.2005.03.011.

McFadden, R.R., Snoke, A.W., and Barnes, C.G., 2006, this volume, Structural and petrologic evolution of the Bear Peak intrusive complex, Klamath Mountains, California, *in* Snoke, A.W., and Barnes, C.G., eds., Geological studies in the Klamath Mountains province, California and Oregon: A volume in honor of William P. Irwin: Boulder, Colorado, Geological Society of America Special Paper 410, doi: 10.1130/2006.2410(16).

Miller, J., Miller, R., Wooden, J., and Harper, G., 2003, Geochronologic links between the Ingalls ophiolite, North Cascades, Washington and the Josephine ophiolite, Klamath Mts., Oregon and California: Geological Society of America Abstracts with Programs, v. 35, p. 113.

Parrish, R.R., Roddick, J.C., Loveridge, W.D., and Sullivan, R.D., 1987, Uranium-lead analytical techniques at the geochronology laboratory, Geological Survey of Canada, *in* Radiogenic age and isotopic studies, Report 1: Ottawa, Geological Survey of Canada Paper 87-2, p. 3–7.

Saleeby, J.B., Harper, G.D., Snoke, A.W., and Sharp, W.D., 1982, Time relations and structural-stratigraphic patterns in ophiolite accretion, west-central Klamath Mountains, California: Journal of Geophysical Research, v. 87, p. 3831–3848.

Schärer, U., 1984, The effect of initial ^{230}Th disequilibrium on young U-Pb ages: The Makalu case, Himalaya: Earth and Planetary Science Letters, v. 67, p. 191–204, doi: 10.1016/0012-821X(84)90114-6.

Scott, D.J., and St-Onge, M.R., 1995, Constraints on Pb closure temperature in titanite based on rocks from the Ungava orogen, Canada: Implication for U-Pb geochronology and P-T-t path determinations: Geology, v. 23, p. 1123–1126, doi: 10.1130/0091-7613(1995)023<1123:COPCTI>2.3.CO;2.

Snoke, A.W., 1977, A thrust plate of ophiolitic rocks in the Preston Peak area, Klamath Mountains, California: Geological Society of America Bulletin, v. 88, p. 1641–1659, doi: 10.1130/0016-7606(1977)88<1641:ATPOOR>2.0.CO;2.

Snoke, A.W., and Barnes, C.G., 2002, Anatexis and dynamothermal metamorphism during the emplacement of a syntectonic oceanic arc-root pluton, Klamath Mountains, California: Geological Society of America Abstracts with Programs, v. 34, no. 5, p. A-22.

Snoke, A.W., and Barnes, C.G., 2006, this volume, The development of tectonic concepts for the Klamath Mountains province, California and Oregon, *in* Snoke, A.W., and Barnes, C.G., eds., Geological studies in the Klamath Mountains province, California and Oregon: A volume in honor of William P. Irwin: Boulder, Colorado, Geological Society of America Special Paper 410, doi: 10.1130/2006.2410(01).

Snoke, A.W., Quick, J.E., and Bowman, H.R., 1981, Bear Mountain igneous complex, Klamath Mountains, California: An ultrabasic to silicic calc-alkaline suite: Journal of Petrology, v. 22, p. 501–552.

Snoke, A.W., Sharp, W.D., Wright, J.E., and Saleeby, J.B., 1982, Significance of mid-Mesozoic peridotitic to dioritic intrusive complexes, Klamath Mountains—western Sierra Nevada, California: Geology, v. 10, p. 160–166, doi: 10.1130/0091-7613(1982)10<160:SOMPTD>2.0.CO;2.

Stacey, J.S., and Kramers, J.D., 1975, Approximation of terrestrial lead isotope evolution by a two-stage model: Earth and Planetary Science Letters, v. 26, p. 207–221, doi: 10.1016/0012-821X(75)90088-6.

Steiger, R.H., and Jäger, E., 1977, Subcommission on geochronology: Convention on the use of decay constants in geo- and cosmochronology: Earth and Planetary Science Letters, v. 36, p. 359–362, doi: 10.1016/0012-821X(77)90060-7.

Taliaferro, N.L., 1942, Geologic history and correlation of the Jurassic of southwestern Oregon and California: Geological Society of America Bulletin, v. 53, p. 71–112.

Verts, L.A., Chamberlain, K.R., and Frost, C.D., 1996, U-Pb sphene dating of metamorphism: The importance of sphene growth in the contact aureole of the Red Mountain pluton, Laramie Mountains, Wyoming: Contributions to Mineralogy and Petrology, v. 125, p. 186–199, doi: 10.1007/s004100050215.

Watson, E.B., and Harrison, T.M., 1983, Zircon saturation revisited: Temperature and composition effects in a variety of crustal magma types: Earth and Planetary Science Letters, v. 64, p. 295–304, doi: 10.1016/0012-821X(83)90211-X.

Wright, J.E., and Fahan, M.R., 1988, An expanded view of Jurassic orogenesis in the western United States Cordillera: Middle Jurassic (pre-Nevadan) regional metamorphism and thrust faulting within an active arc environment, Klamath Mountains, California: Geological Society of America Bulletin, v. 100, p. 859–876, doi: 10.1130/0016-7606(1988)100<0859:AEVOJO>2.3.CO;2.

Zartman, R.E., and Doe, B.R., 1981, Plumbotectonics—The model: Tectonophysics, v. 75, p. 135–162, doi: 10.1016/0040-1951(81)90213-4.

Manuscript Accepted by the Society 10 January 2006

Printed in the USA